



Extreme convection in subtropical South America: TRMM observations and high-resolution modeling

Kristen L. Rasmussen¹, Robert A. Houze, Jr.¹, and Anil Kumar²

¹Department of Atmospheric Sciences, University of Washington, Seattle, WA ★ ²NASA Goddard Space Flight Center, Greenbelt, MD

2012 AGU Fall Meeting
San Francisco, CA
December 5, 2012



Introduction

- Observations from the *Tropical Rainfall Measuring Mission* (TRMM) satellite have led to the realization that intense deep convective storms just east of the Andes in subtropical South America are among the most intense anywhere in the world (Zipser et al. 2006)

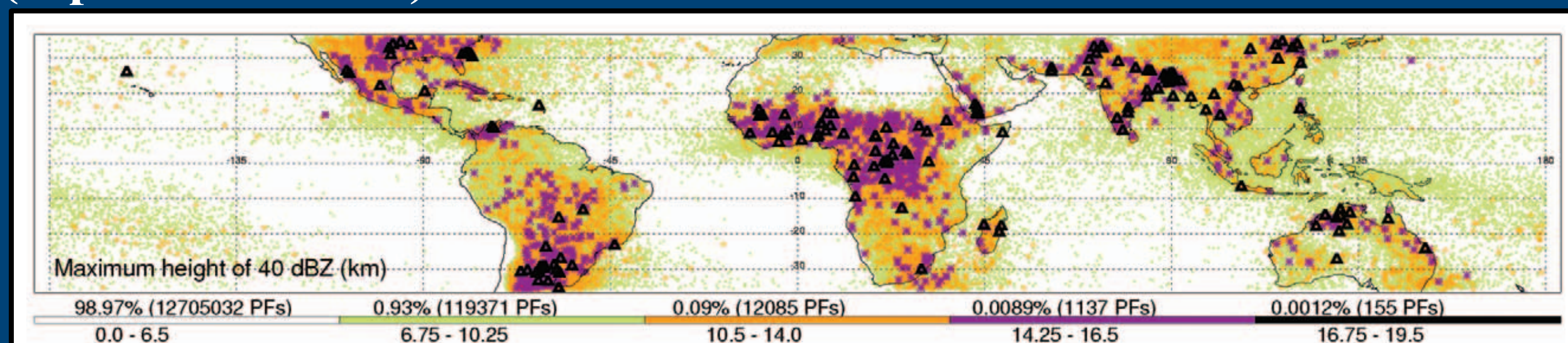


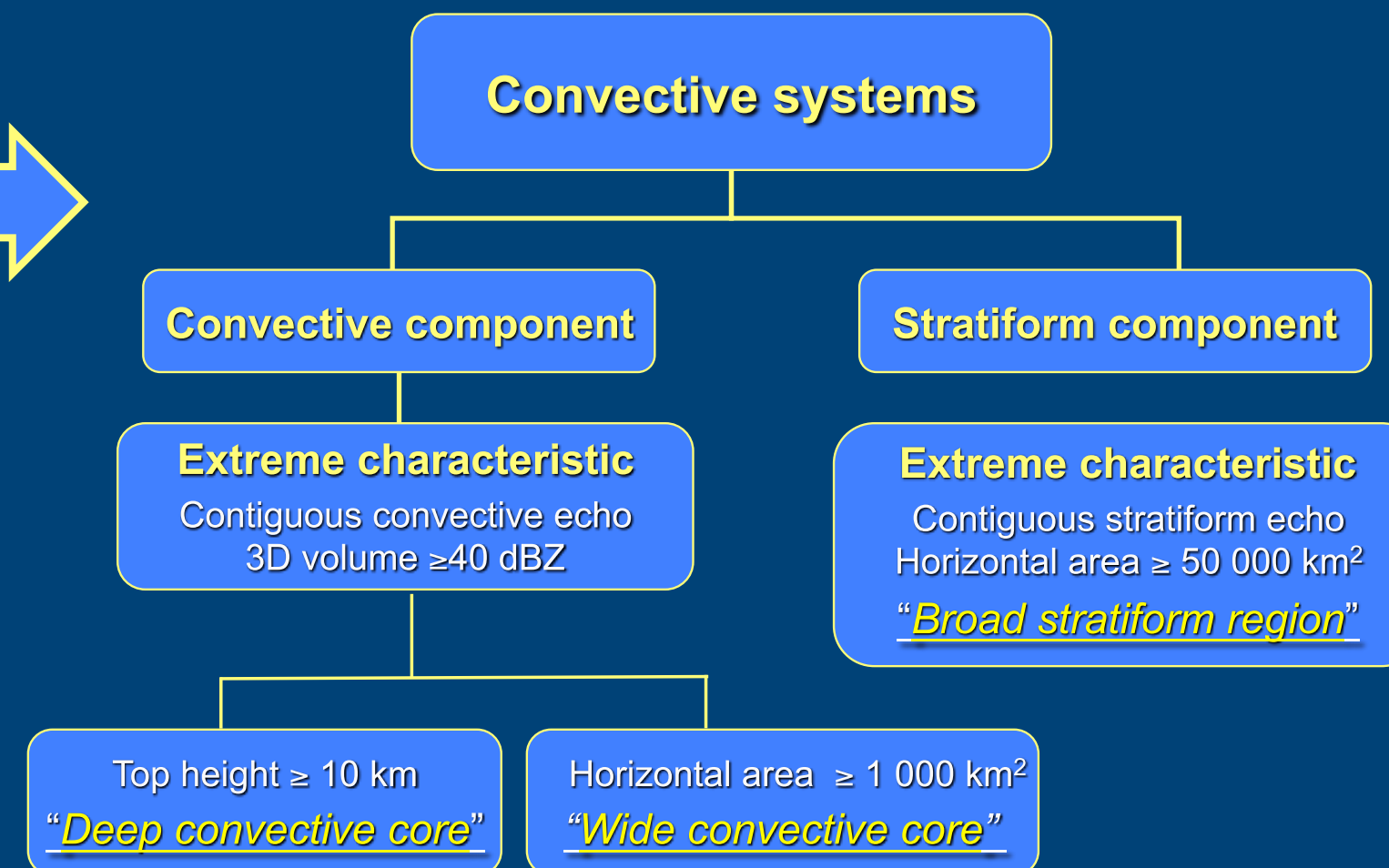
Figure 1. Locations of intense convective events using the color code matching their rarity. From Zipser et al. (2006).

- On average, South American MCC cloud shields are 60% larger than those over the United States (Velasco and Fritsch 1987), the convection is deeper (Zipser et al. 2006), and they have larger precipitation areas than those over the United States or Africa (Durkee et al. 2009)
- Despite the severity and intensity of the storms, relatively few studies have been conducted on South American convection, especially in the lee of the Andes

Background

UW methodology to separate TRMM Precipitation Radar (PR) echoes into three storm types (Houze et al. 2007): *deep convective cores*, *wide convective cores*, and *broad stratiform regions*

- South Asia: Houze et al. (2007), Romatschke et al. (2011a, b)
- South America: Romatschke et al. (2010), Rasmussen and Houze (2011)



Storm evolution hypothesis presented in Romatschke and Houze (2010) and Rasmussen and Houze (2011):

- Deep convective cores* initiate along Andes foothills and secondary topo features
- Convection grows upscale, develops *wide convective cores*, and moves eastward
- Decaying convective elements move farther eastward and develop *broad stratiform regions*

The Andes Mountains funnel warm and moist air southward via the South American Low Level Jet

Analogous environmental setup for deep convection observed near other major mountain ranges (Rocky Mountains and Himalayas)!

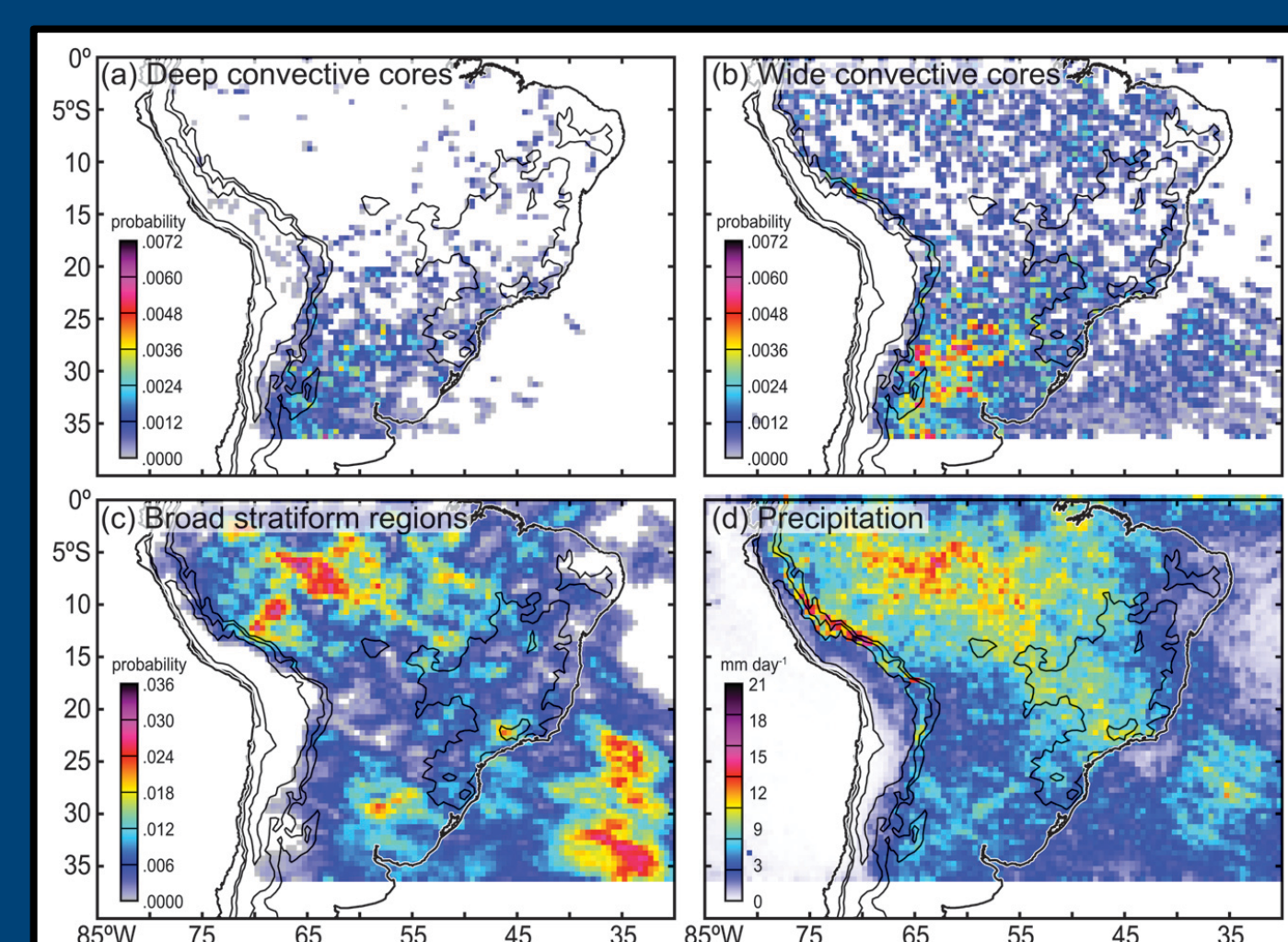


Figure 2. Locations of storm types in South America derived from TRMM PR data. From Romatschke and Houze (2010).

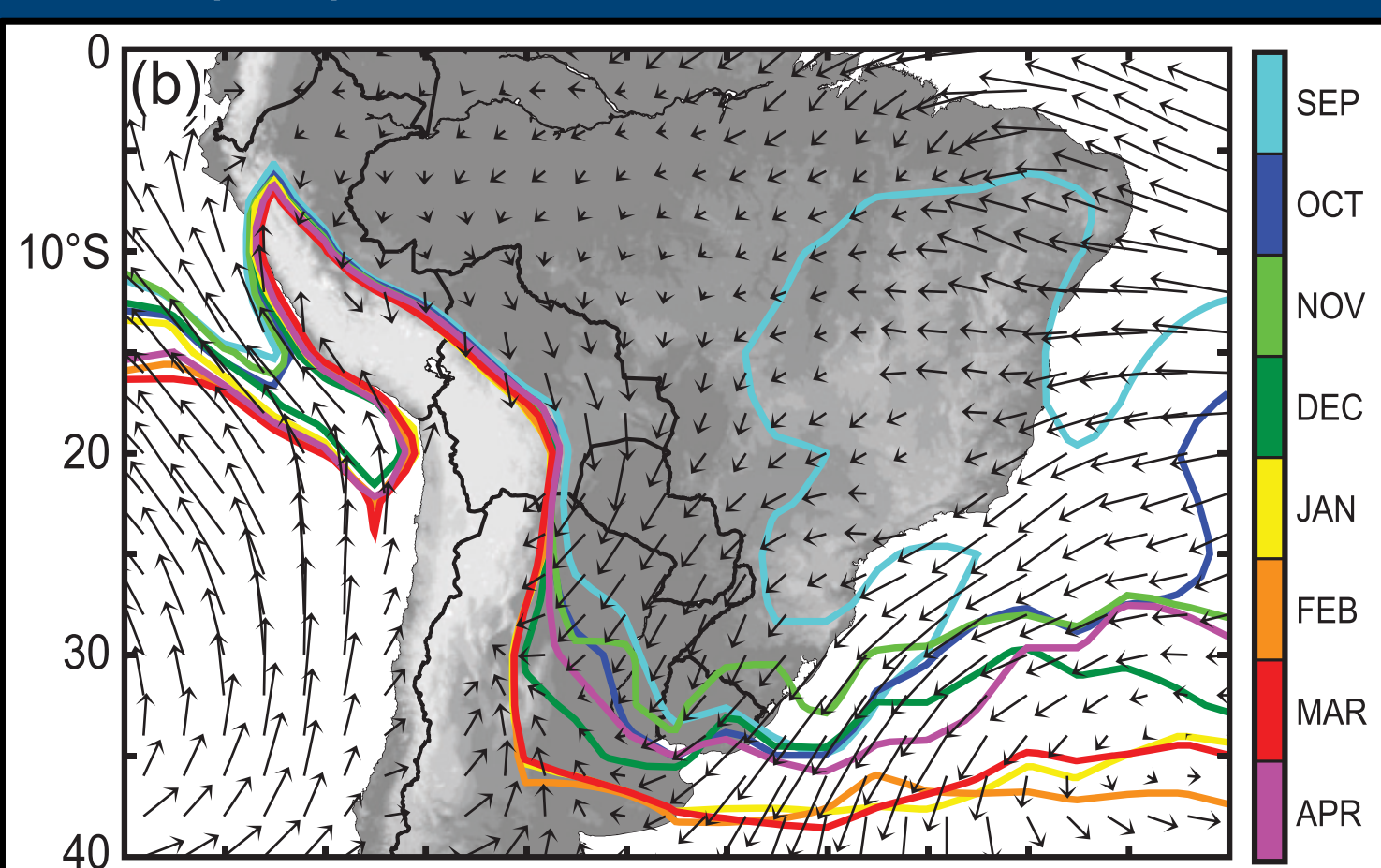


Figure 3. Seasonal progression of moisture (28 mm precipitable water). From Rasmussen and Houze (2011)

South American MCSs

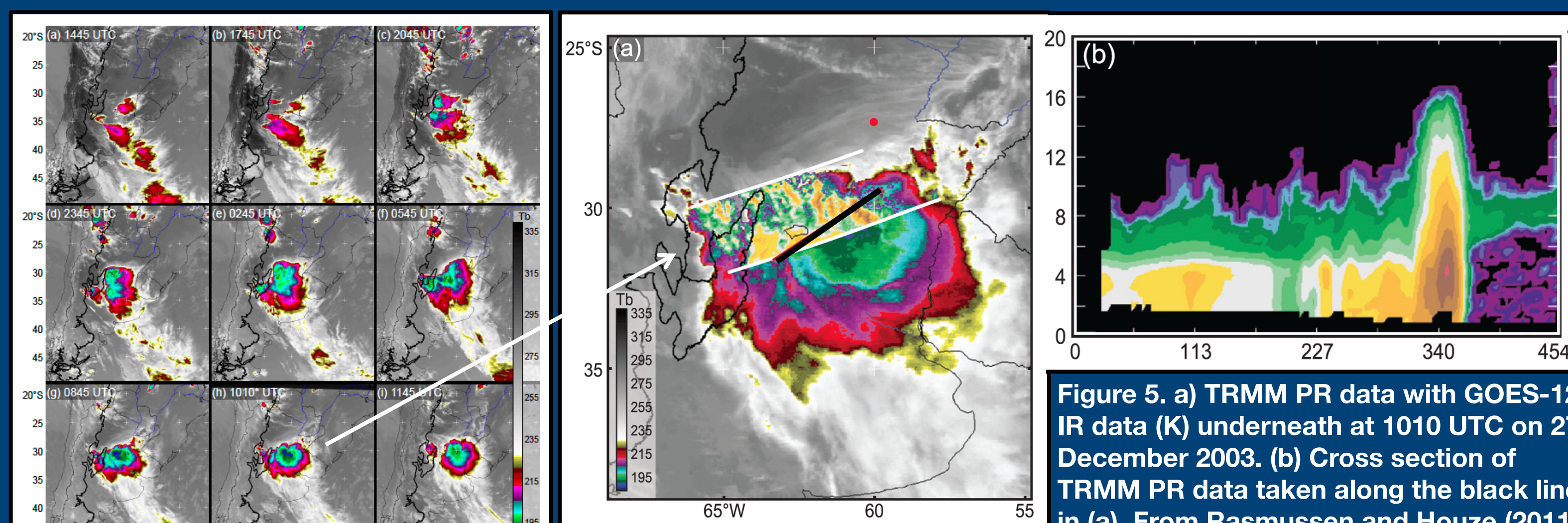


Figure 4. Sequence of infrared satellite images (K) showing storm initiation and evolution for the 26-27 December 2003 wide convective core. From Rasmussen and Houze (2011).

- Strong influence of the Andes foothills and the Sierras de Córdoba Mountains in convective initiation and maintenance of MCSs
- Storms with *wide convective cores* tend to be linearly organized
- Pattern of leading convective line and trailing stratiform precipitation in *wide convective core* storms

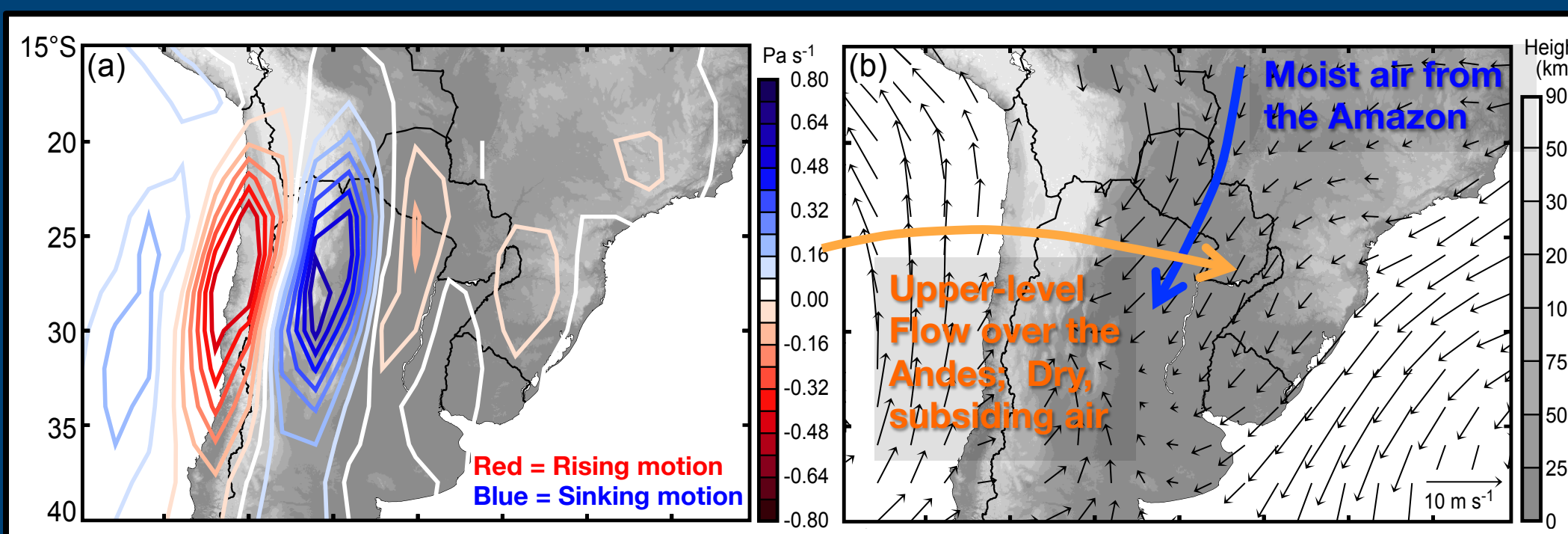


Figure 6. Climatological composite maps for days on which the TRMM PR showed storms containing wide convective cores over subtropical S. America. (a) Vertical motion (omega) and (b) 1000 mb winds. From Rasmussen and Houze (2011).

← Composite maps for days when TRMM observed a *wide convective core* show mid-level subsidence and low-level convergence in the lee of the Andes (Figure 6)

Mesoscale Organization

- Storms with *wide convective cores* tend to be linearly organized
- Similarity to leading-line/trailing-stratiform archetype identified in the United States (Houze et al. 1990; adapted for South America in Fig. 7)

| Degree of Organization | Range of Scores | South America (Rasmussen and Houze 2011) | Oklahoma (Houze et al. 1990) | Switzerland (Schiesler et al. 1995) |
|---------------------------------|-------------------|--|------------------------------|-------------------------------------|
| Strongly Classifiable | $C > 5$ | 11 (20%) | 14 (22.2%) | 0 (0%) |
| Moderately Classifiable | $0 \leq C \leq 5$ | 30 (54.5%) | 18 (28.6%) | 12 (21.4%) |
| Weakly Classifiable | $C < 0$ | 7 (12.7%) | 10 (15.9%) | 18 (32.1%) |
| All Classifiable Systems | All C | 48 (87.3%) | 42 (66.7%) | 30 (53.6%) |
| All Unclassifiable Systems | --- | 7 (12.7%) | 21 (33.3%) | 26 (46.4%) |
| Total Number of Storms Analyzed | --- | 55 | 63 | 56 |

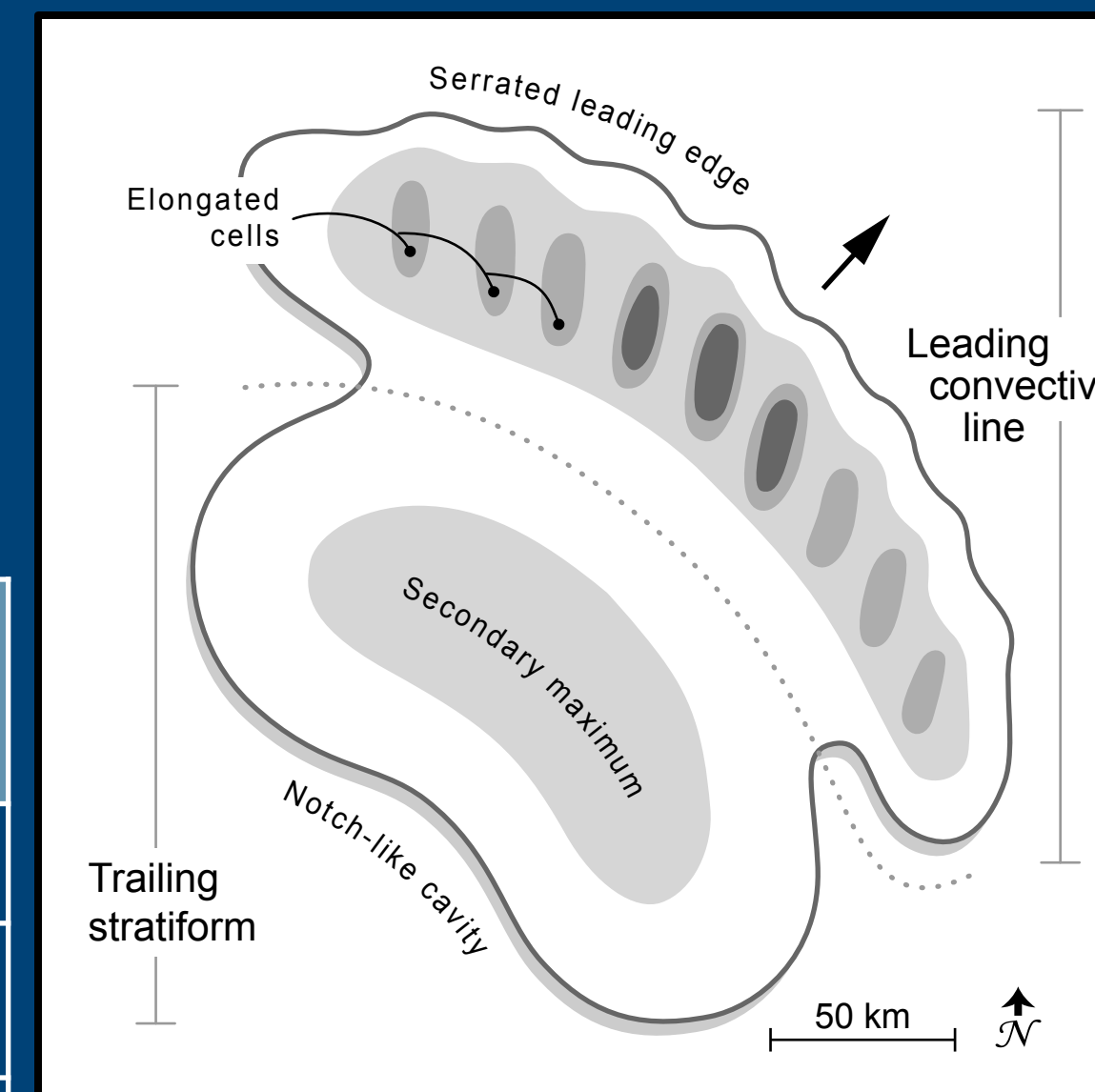


Figure 7. Schematic of the leading-line/trailing stratiform archetype described in Houze et al. (1990), but reoriented for study in the Southern Hemisphere. Increasing levels of shading indicate more intense radar reflectivity. Storms with *wide convective cores* were systematically compared to this idealized structure. From Rasmussen and Houze (2011).

★ Storms with wide convective cores in subtropical South America tend to be line-organized and are similar in organization to squall lines in Oklahoma ★

High-Resolution Modeling Study

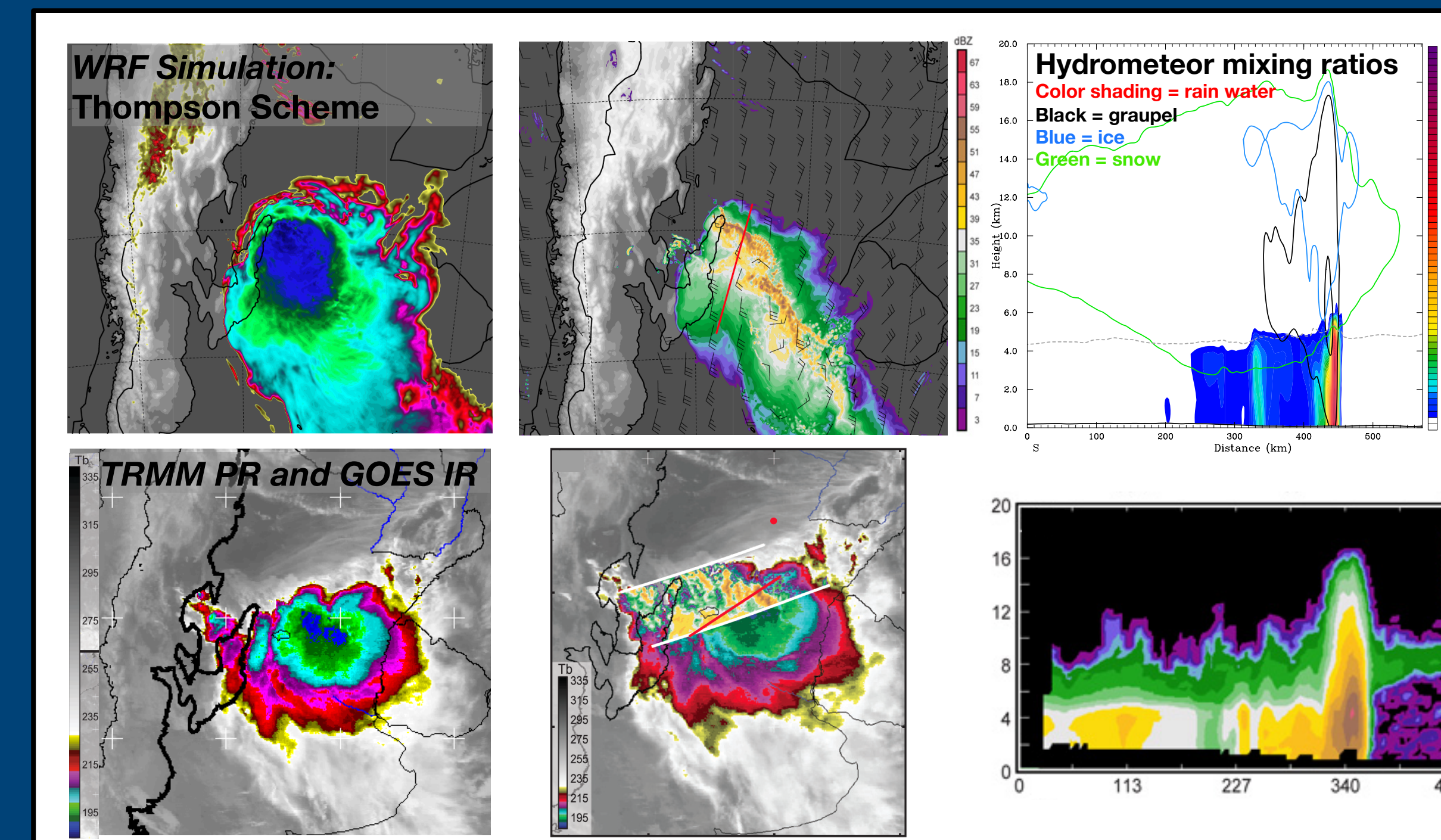


Figure 8. Comparison of a WRF simulation (top row) to TRMM PR and GOES data (bottom row).

← WRF simulations have produced an excellent representation of the 27 December 2003 case study from Rasmussen and Houze (2011)

← Microphysics testing indicated that the Thompson scheme captures leading-line/trailing stratiform structure

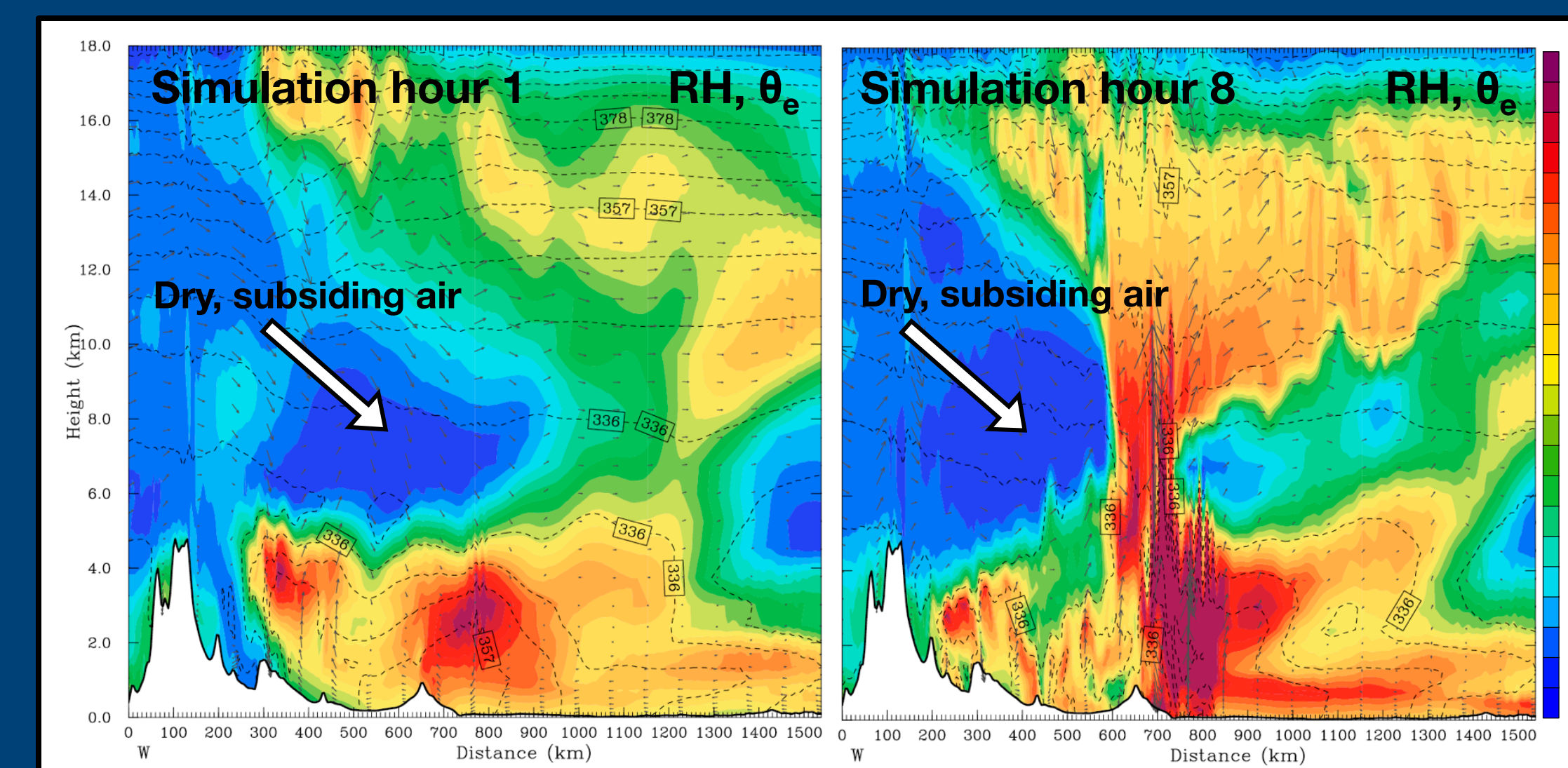


Figure 9. Vertical cross-sections from the WRF simulation at 30° S. Shading indicates relative humidity, the dashed contours are equivalent potential temperature, and the vectors are circulation winds in the plane.

← WRF simulation confirms the lee subsidence hypothesis presented in Rasmussen and Houze (2011)

Conclusions

- Deep convection initiates near the Sierras de Córdoba Mountains and Andes foothills, grows upscale into eastward propagating MCSs, and decays into stratiform regions
- Storms with wide convective cores in subtropical South America tend to be line-organized and are similar in organization to squall lines in Oklahoma
- Lee subsidence capping low-level moisture is observed in the model results
- Choice of microphysics scheme can greatly impact the storm structure and is important for deep convective simulations

Acknowledgements

This research was supported by:
National Aeronautics and Space Administration Grants NNX10AH70G and NNX11AL65H
National Science Foundation Grants ATM-0820586 and AGS-1144105